SUPPLEMENTARY INFORMATION FOR:

Molecular architecture of the *Legionella* Dot/Icm type IV secretion system

Debnath Ghosal[1], Yi-Wei Chang[1], Kwang Cheol Jeong[2,3], Joseph P. Vogel[2], Grant J. Jensen[1,4]

Figure S1. Local resolution of subtomogram averages. A) WT Dot/Icm complex, B) DotF-sfGFP stabilized Dot/Icm complex.

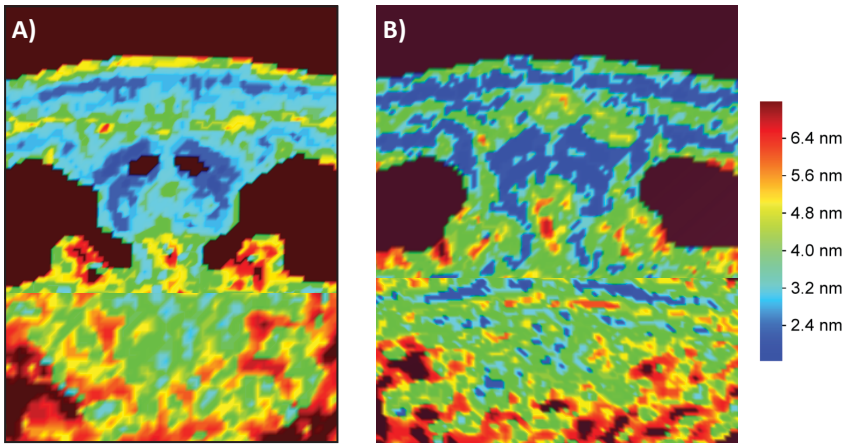

Figure S2 Cytoplasmic densities in DotF-sfGFP map. A-D) Tomographic slices through back, middle, and front planes of the cytoplasmic densities. OM = outer membrane; IM = inner membrane. Arrow indicates additional density directly below the short central barrel. Scale bar 10 nm.

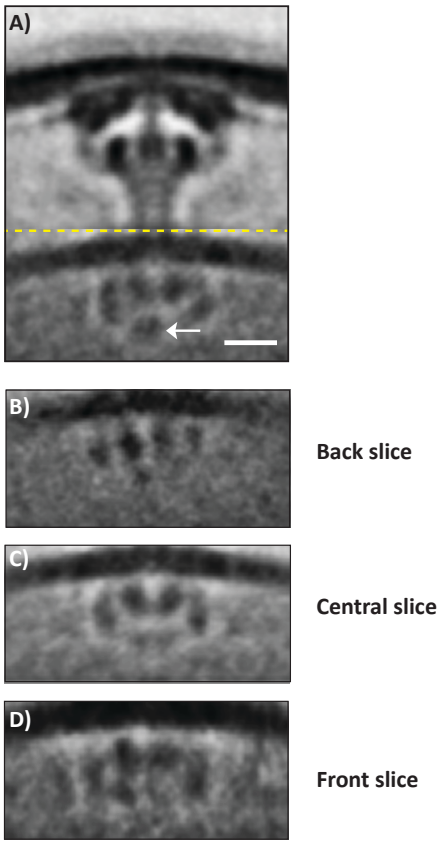

Figure S3. Confirmation of *L. pneumophila* strains. Western blots with the indicated Dot-specific antibodies. ICDH, a cytoplasmic house-keeping protein, was used as a loading control for each set of blots. Samples were loaded in the following order: A) 1. Lp02 (wild-type), 2. JV5319 (*SΔ(UF)*), 3. JV9114 (*DotC-sfGFP*), 4. JV9082(*DotF-sfGFP*), B) 1. Lp02 (wild-type), 2. JV5319 (*SΔ(UF)*), 3.JV7058 (*ΔdotF ΔdotG ΔdotH*),4. JV5460 (*SΔ(UF) + dotCDH*), 5. JV5443 (*SΔ(UF) + dotCDFGH*), and C) 1. Lp02 (wild-type),2. JV5319 (*SΔ(UF)*), 3. JV918 (*ΔdotB*), 4. JV2422 (*ΔdotA ΔdotL*), 5. JV1644(*ΔdotO*), 6. JV6781 (*ΔdotB ΔdotL ΔdotO*). Similar blots are already published for other mutants [22,28,36,67].

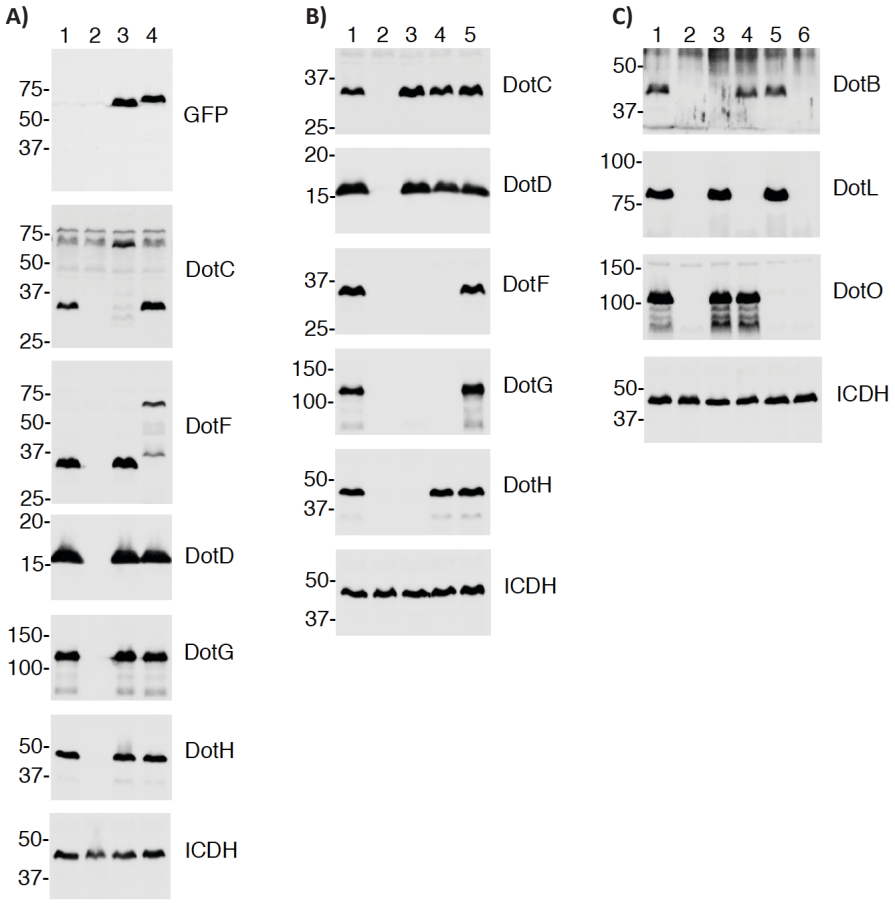

Figure S4 Domain structures of proteins considered here. (see legend next page)

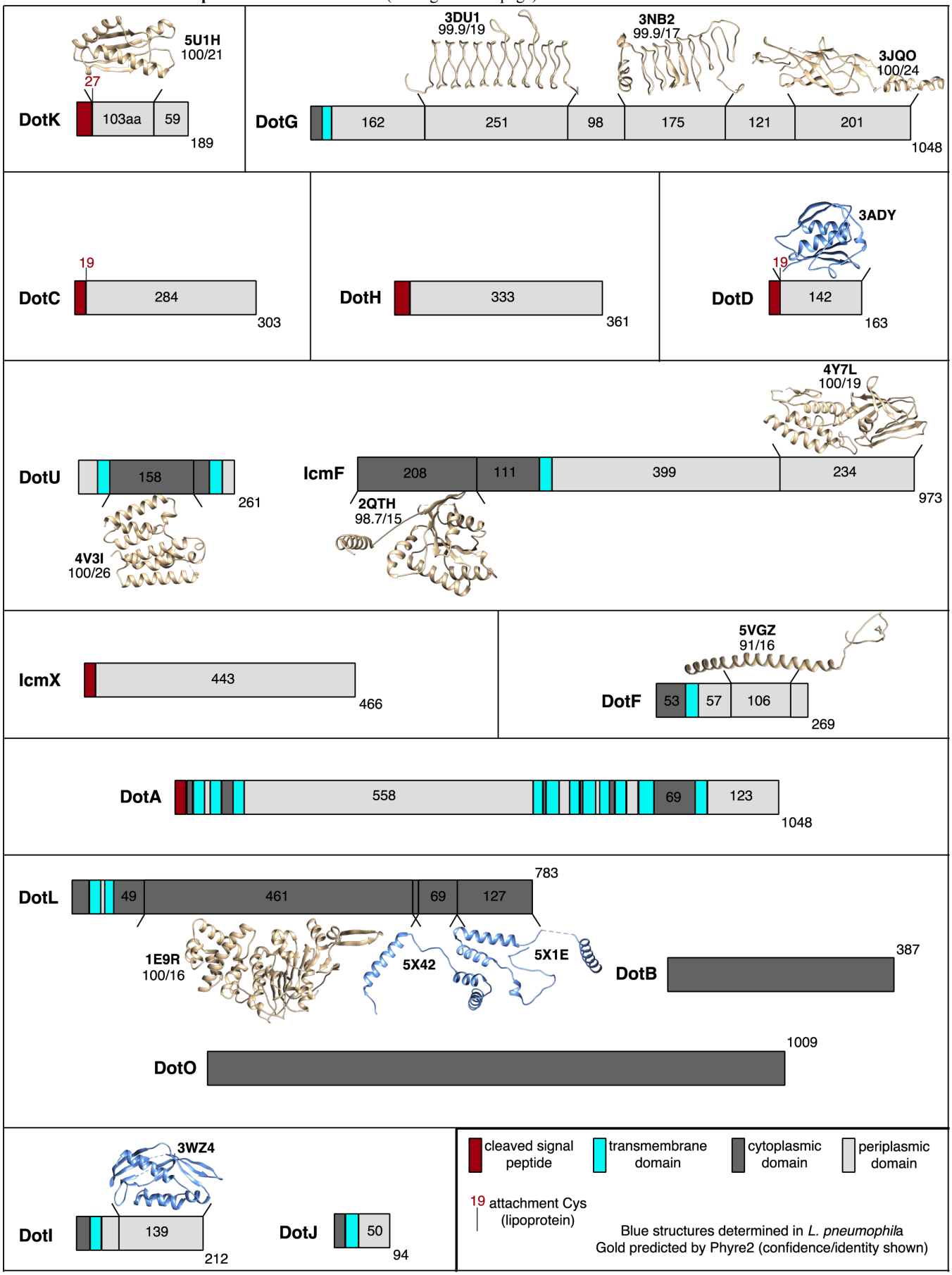

Figure S5. Domain structures of components not treated in this study. Predicted domains are shown from N- (left) to C-terminus (right). Red = cleaved signal peptide, cyan = transmembrane domain, dark gray = cytoplasmic domain, light gray = periplasmic domain. Domains whose structure has been solved (blue) or predicted with high confidence (gold) are indicated. In each case, the structure (with PDB ID, and confidence/sequence identity for Phyre2 predictions) is shown above the domain if periplasmic and below if cytoplasmic. The length of key domains is indicated, with total protein length listed at the C-terminus. The locations of cysteines in lipoproteins that are linked to the OM are noted in red.

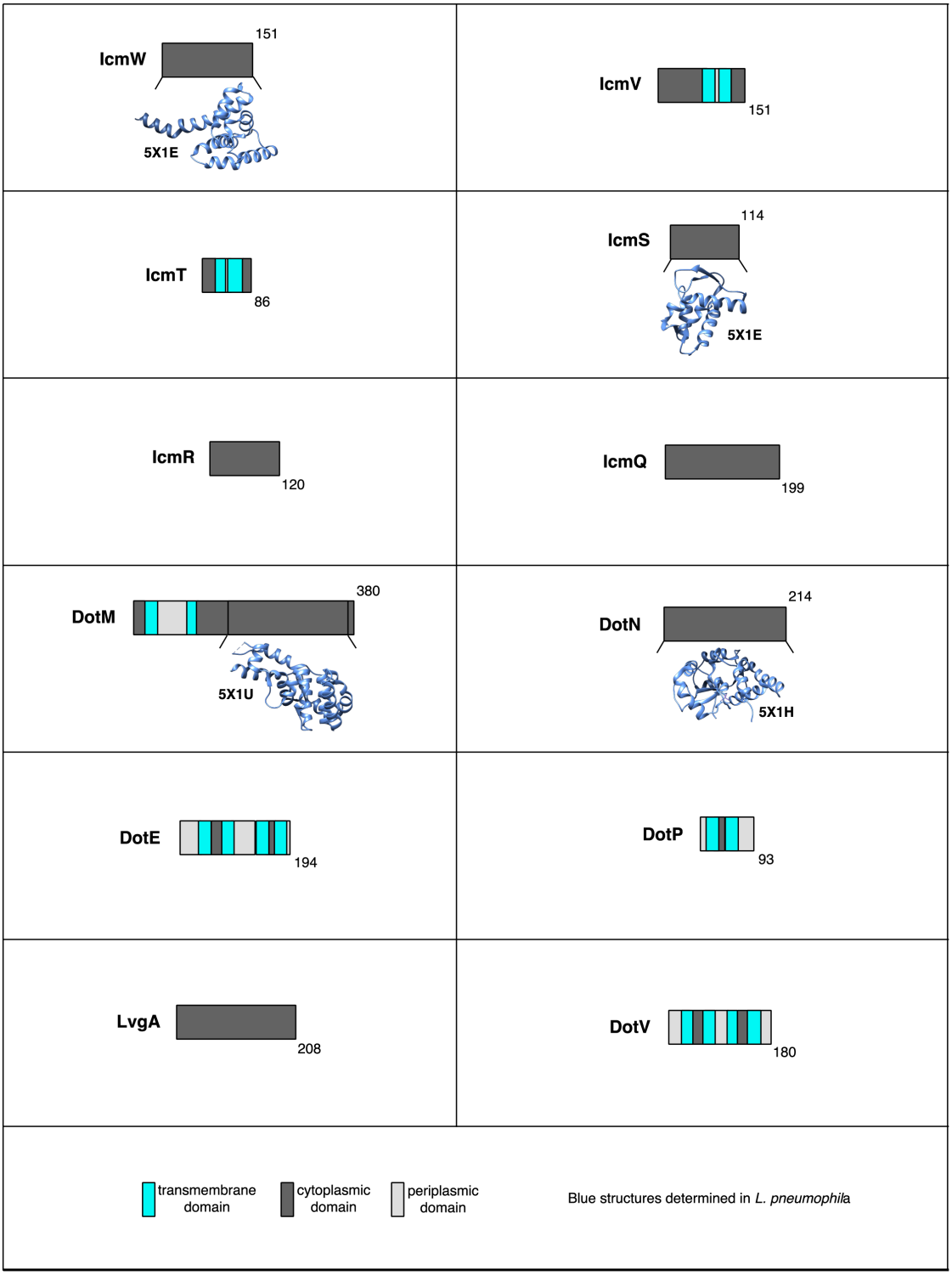

Figure S6. The Dot/Icm complex is composed of several stacked ring-like structures. A) OM-associated DotG TrbI-ring (red dotted line), DotK-ring (green dotted line), DotD/H-ring (salmon and grey dotted lines), periplasmic DotC/H-ring (cyan and salmon dotted lines), and DotG beta-helix ring (red dotted line) and an IM- associated DotI ring (pink dotted line). B) A top-view of the TrbI ring formed by VirB10 in the VirB7/9/10 complex (3JQO). C) Cross-section of the periplasmic channel formed by the DotG repeat region with an inner lumen diameter of ~4 nm and an outer diameter of ~8.5 nm. Outer and inner diameters of a 13-mer ring are consistent with the channel width seen in the subtomogram average. D) Example DotI 12-mer with same binding interface as in crystal structures showing one plausible way a 12-mer could form a ring of the size seen in the ECT map. C and D were generated by the SymmDock server. Scale bar 10 nm (A).

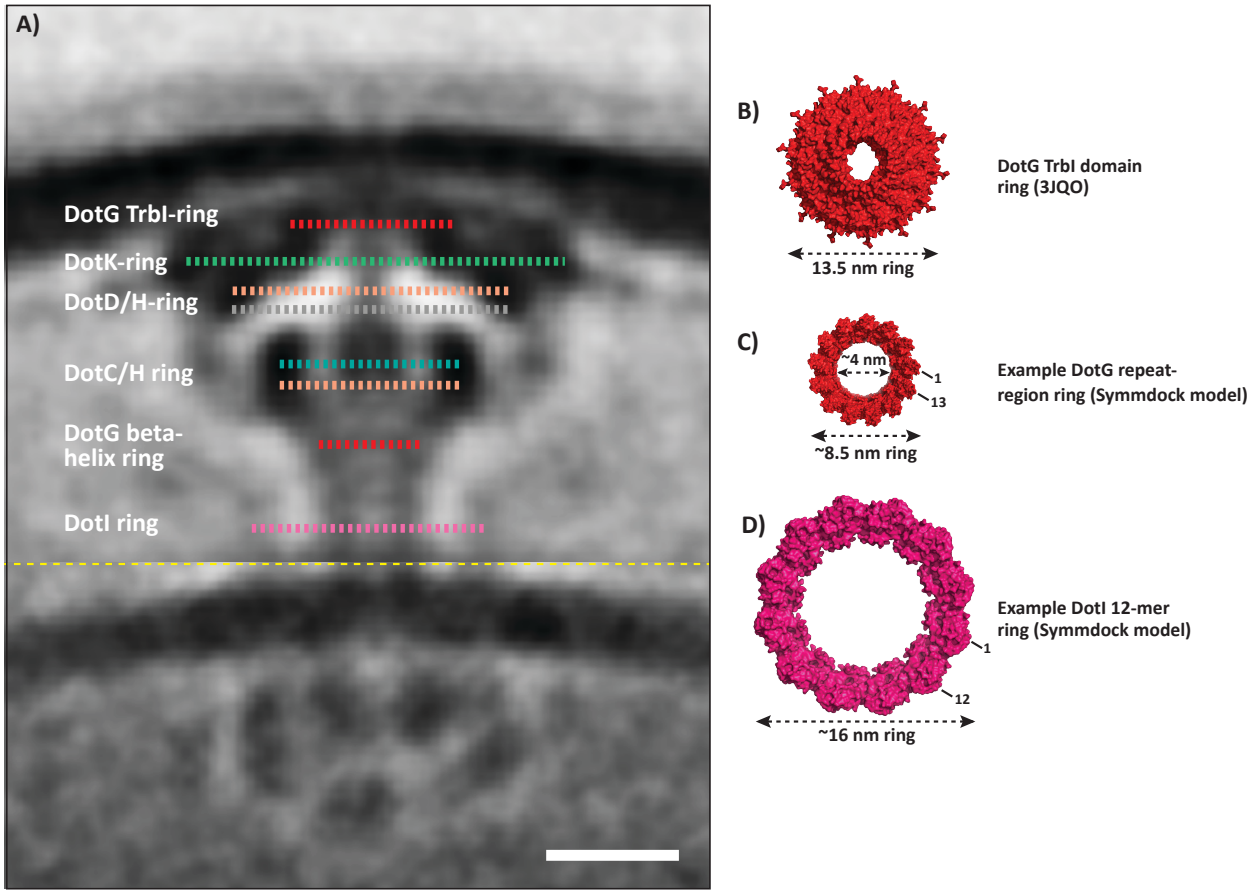

Figure S7. Beta and gamma densities are present in WT, reconstituted DotCDH (+DotU/IcmF) and reconstituted DotCDHFG (+DotU/IcmF) complexes. Gamma densities in individual particles of the reconstituted DotCDH (+DotU/IcmF) complex are comparable to those of the reconstituted DotCDHFG (+DotU/IcmF) complex and the WT complex. However, due to flexibility, they appear less pronounced in the reconstituted DotCDH (+DotU/IcmF) average.

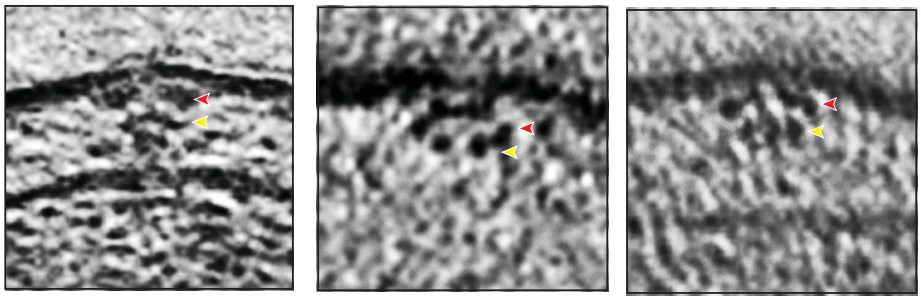

Figure S8. Secondary structure predictions of DotH. A) Prediction of DotH structure using I-TASSER suggests that DotH includes two or more separate domains. B) DotH and VirB9 are suggested to be counterparts. VirB9 in the T4ASS also has two separate domains that extend between the O-layer and the I-layer. C) DotH's predicted structure fits well in the Dot/Icm complex. Circumstantial evidence suggests that DotH would extend between the beta and the gamma densities along the elbow very much like VirB9. D) Secondary structure predictions of VirB9 and DotH also suggest they might assume a similar fold.

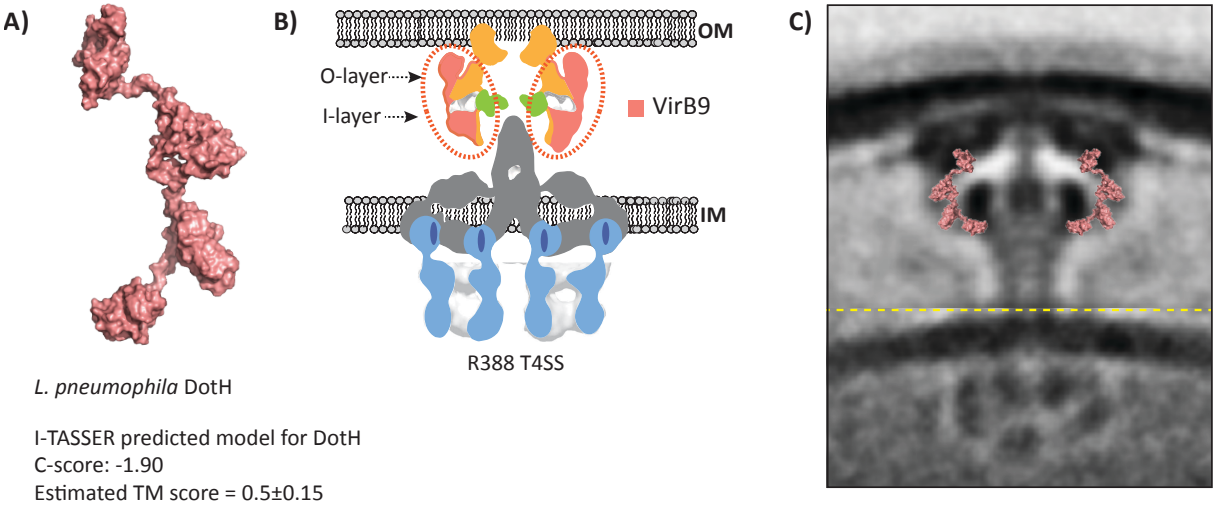

D) VirB9 (Plasmid R388 T4SS)

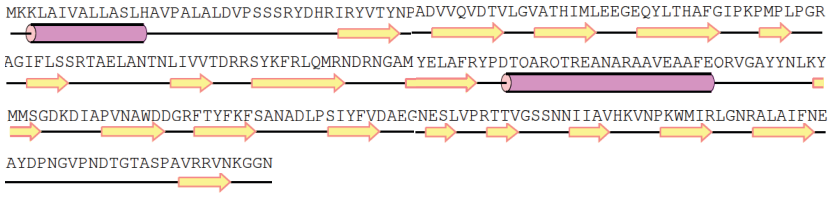

DotH (*L. pneumophila* Dot/Icm T4BSS)

Figure S9. **Positioning of DotD's N0 domain.** A) Overlaying the *X. citri* VirB7/9 complex (2N01) on the pKM101 VirB7/9/10 OM complex (3JQO) indicates that the *X. citri* VirB7-N0 domain would be at the periphery of the OM complex. Since VirB7 and DotD are counterparts and DotD also has an N0 domain, we propose that DotD's N0 domain would occupy a very similar position as *X. citri* VirB7's N0 domain. B) Comparing the lipidation residue, and length of DotD's N-terminal disordered region and *X. citri* VirB7/VirB9 interaction interface, we propose that DotD's N0 domain will be 3.5 nm or less away from the hat. The only unaccounted-for density within that distance from the peripery of the hat is the beta density. The beta densities form a ring of diameter ~23 nm. C) A very similar diameter ring was proposed by Souza et al. for the *X. citri* VirB7-N0 domain. D) Crystal structure of the *L. pneumophila* DotD N0 domain. A) Scale bar 10 nm.

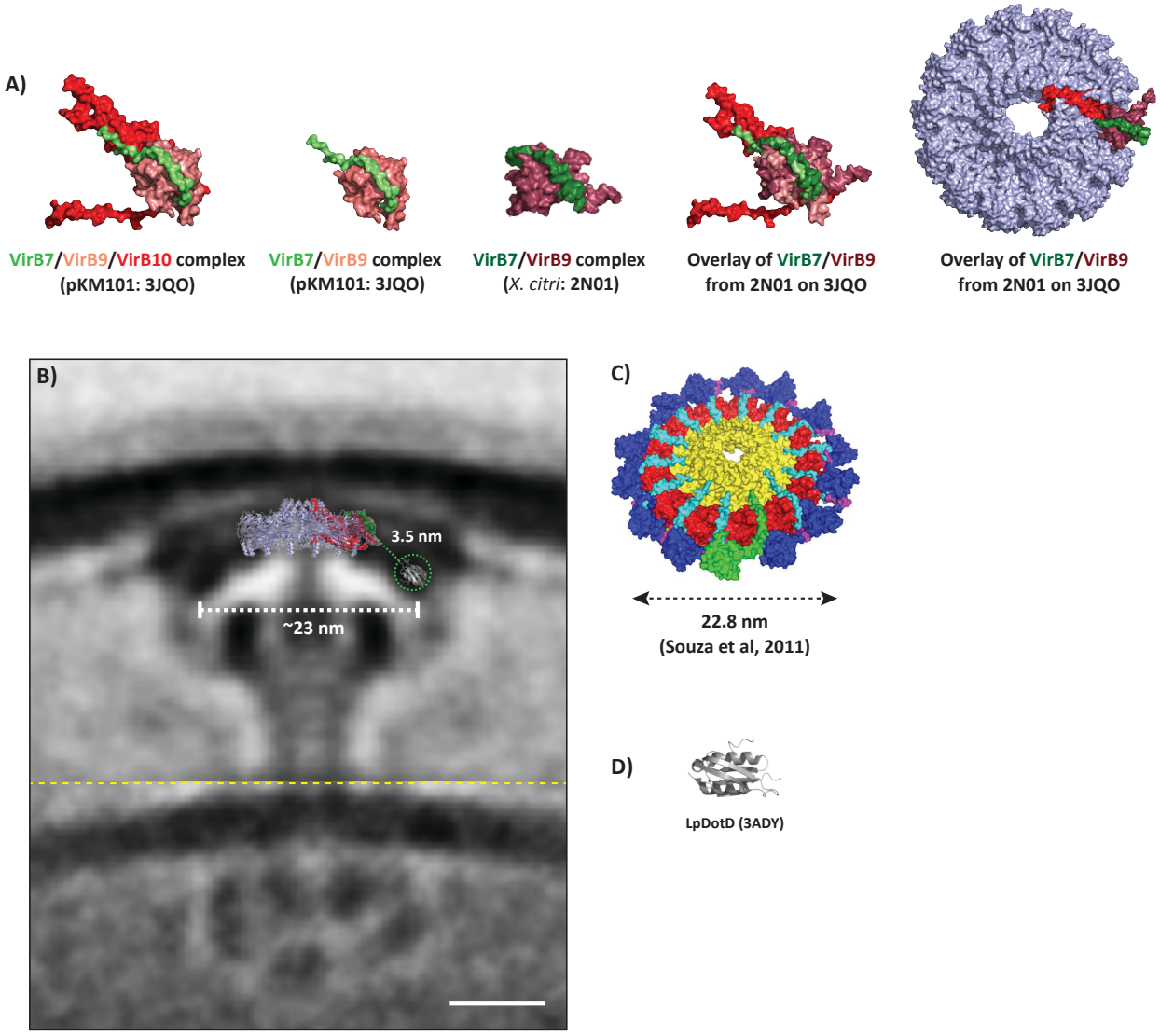

Figure S10. Flexibility and identification of the wings as DotF. A-H) Tomographic slices through wild-type T4BSSs showing wing densities (circled in blue) in various locations with respect to the membranes and the rest of the T4BSS. I) Average of the wild-type T4BSS, with yellow and red arrows and yellow circles as in individual particles for positional reference. Scale bar 10 nm. J-N) Central slices through sub-tomogram averages of various strains with particles aligned on the region of the wing density (between IM and gamma ring). Yellow circles indicate presence of wings, white circles indicate absence.

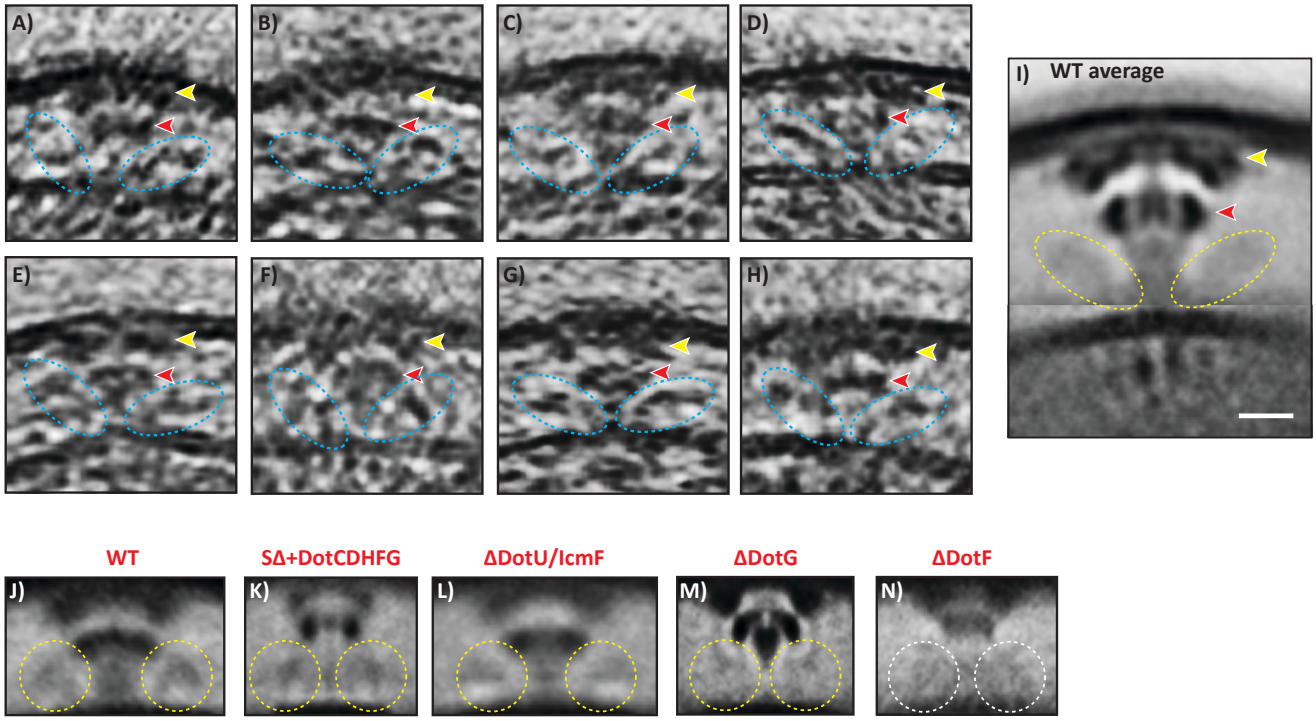

Figure S11. DotI forms a ring around the central channel at the base of the wings and is required to recruit the cytoplasmic ATPases. All panels except K and N: Central tomographic slices through various structures. A-D) Unannotated and (E-H) annotated central slices with the shape of the IM indicated, showing that loss of the cytoplasmic ATPases (in Δ*dotIJ* and Δ*dotLOB* structures) correlates with a pronounced puckering of the membrane. K and N) Central slices through the indicated difference maps. Note that all averages shown are from particles aligned on the IM-associated densities. White circles in I-N) indicate the location of the DotI ring at the base of the wings, present in wild-type and DotF-sfGFP but absent in Δ*dotIJ*. Yellow circles surround the densities due to the cytoplasmic ATPases, also present in wild-type and DotF-sfGFP but absent in Δ*dotIJ*. Rectangles in N) indicate paired positive and negative differences resulting in a change in the shape of the membrane. Note other missing densities in the upper periplasm cannot be DotI, as it is held close to the IM by its transmembrane helix.

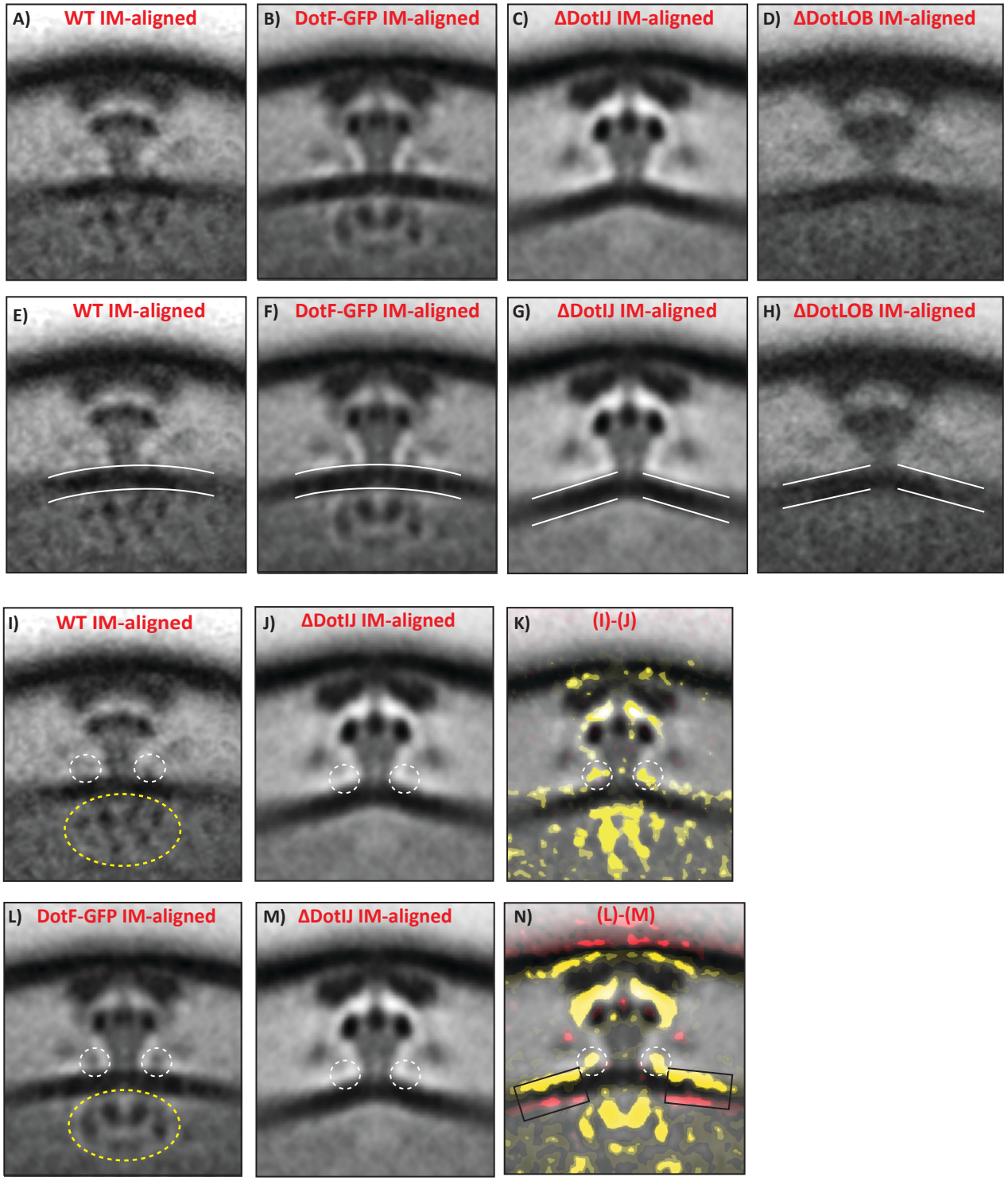

Table 1

No	Strain name	Description	No of tomograms collected	No of particles used for subtomogram averaging
1	Lp02	*Legionella pneumophila thyA* (WT)	188	386
2	JV4404	*Legionella pneumophila thyA ΔdotA/icm*	80	NA
3	JV2422	*Legionella pneumophila thyA ΔdotA ΔdotL*	77	195
4	JV3559	*Legionella pneumophila thyA ΔdotG*	164	321
5	JV3563	*Legionella pneumophila thyA ΔdotH*	63	NA
6	JV3572	*Legionella pneumophila thyA ΔdotD*	121	NA
7	JV3579	*Legionella pneumophila thyA ΔdotF*	181	212
8	JV3743	*Legionella pneumophila thyA ΔdotC*	65	NA
9	JV9114	*Legionella pneumophila thyA dotC-gfp*	117	375
10	JV6781	*Legionella pneumophila thyA ΔdotLOB*	109	367
11	JV5443	*Legionella pneumophila* (JV4404+ *dotCDHFG*)+ *icmF/dotU*	113	261
12	JV7967	*Legionella pneumophila thyA ΔdotI ΔdotJ*	87	348
13	JV5460	*Legionella pneumophila thyA* (JV4404+ *dotCDH*)+ *icmF/dotU*	99	201
14	JV2067	*Legionella pneumophila thyA ΔicmX*	101	309
15	JV3588	*Legionella pneumophila thyA ΔdotK*	107	244
16	JV1180	*Legionella pneumophila thyA ΔdotUF*	262	280
17	JV1181	*Legionella pneumophila thyA ΔdotUF*	223	378
18	JV9082	*Legionella pneumophila thyA dotF-sfGFP*	75	230
19	JV7091	*Legionella pneumophila ΔdotE ΔdotP*	49	405

Table 2. Bacterial strains, plasmids, and primers employed in this study

Strain, plasmid or primer	Relevant properties	Reference or source
L. pneumophila		
Lp02	Philadelphia-1 *thyA, hsdR, rpsL*	Berger 1993
JV918	Lp02 Δ*dotB*	Vincent 2006
JV1180	Lp02 Δ*dotU* Δ*icmF*	Sexton 2004
JV1181	Lp02 Δ*dotU* Δ*icmF*	Sexton 2004
JV1644	Lp02 Δ*dotO*	Vincent 2006
JV2067	Lp02 Δ*icmX*	Vincent 2006
JV2422	Lp02 Δ*dotA* Δ*dotL*	Vincent 2006
JV3559	Lp02 Δ*dotG*	Vincent 2006
JV3563	Lp02 Δ*dotH*	Vincent 2006
JV3572	Lp02 Δ*dotD*	Vincent 2006
JV3579	Lp02 Δ*dotF*	Vincent 2006
JV3588	Lp02 Δ*dotK*	Vincent 2006
JV3743	Lp02 Δ*dotC*	Vincent 2006
JV4044	Lp02 super *dot*/*icm* deletion Δ*dotU* Δ*icmF*	Vincent 2006
JV5319	Lp02 super *dot*/*icm* deletion *dotU*+ *icmF*+	Vincent 2006
JV5443	JV5319 + pJB4027 (SΔ(UF) + *dotDCHGF*)	Ghosal 2017
JV5460	JV5319 + pJB4417 (SΔ(UF) + *dotDCH*)	Jeong submitted
JV5629	Lp02 Δ*dotL* Δ*dotB*	Vincent 2006
JV6781	Lp02 Δ*dotL* Δ*dotO* Δ*dotB*	This study
JV7967	Lp02 Δ*dotI* Δ*dotJ*	This study
JV7058	Lp02 Δ*dotH* Δ*dotG* Δ*dotF*	This study
JV7091	Lp02 Δ*dotE* Δ*dotP*	This study
JV9082	Lp02 DotF-sfGFP integrated on chromosome	This study
JV9114	Lp02 DotC-sfGFP integrated on chromosome	This study
Plasmids		
pJB908	RSF1010 cloning vector	Sexton 2004
pJB1001	Δ*dotL* suicide plasmid	Buscher 2005
pJB1333	Δ*dotO* suicide plasmid	Vincent 2006
pJB1555	*dotH* complementing clone	This study
pJB4417	*dotD dotC dotH* complementing clone	This study
pJB5184	Δ*dotH* Δ*dotG* Δ*dotF* suicide plasmid	This study
pJB5185	Δ*dotE* Δ*dotP* suicide plasmid	This study
pJB6162	Δ*dotJ* Δ*dotI* suicide plasmid	This study
pJB7255	DotF-sfGFP integration plasmid	This study
pJB7264	DotC-sfGFP with SacB/CmR cassette	This study
pJB7283	DotC-sfGFP integration plasmid	This study
pSR47S	R6K suicide vector	Merriam 1997